OPEN ACCESS Freely available online

PLOS ONE

The Potential and Flux Landscape Theory of Ecology

Li Xu[1☯], Feng Zhang[1,2☯], Kun Zhang[1], Erkang Wang[1], Jin Wang[1,2,3*]

1 State Key Laboratory of Electroanalytical Chemistry, Changchun Institute of Applied Chemistry, Chinese Academy of Sciences, Changchun, Jilin, China, **2** College of Physics, Jilin University, Changchun, Jilin, China, **3** Department of Chemistry & Physics, State University of New York at Stony Brook, Stony Brook, New York, United States of America

Abstract

The species in ecosystems are mutually interacting and self sustainable stable for a certain period. Stability and dynamics are crucial for understanding the structure and the function of ecosystems. We developed a potential and flux landscape theory of ecosystems to address these issues. We show that the driving force of the ecological dynamics can be decomposed to the gradient of the potential landscape and the curl probability flux measuring the degree of the breaking down of the detailed balance (due to in or out flow of the energy to the ecosystems). We found that the underlying intrinsic potential landscape is a global Lyapunov function monotonically going down in time and the topology of the landscape provides a quantitative measure for the global stability of the ecosystems. We also quantified the intrinsic energy, the entropy, the free energy and constructed the non-equilibrium thermodynamics for the ecosystems. We studied several typical and important ecological systems: the predation, competition, mutualism and a realistic lynx-snowshoe hare model. Single attractor, multiple attractors and limit cycle attractors emerge from these studies. We studied the stability and robustness of the ecosystems against the perturbations in parameters and the environmental fluctuations. We also found that the kinetic paths between the multiple attractors do not follow the gradient paths of the underlying landscape and are irreversible because of the non-zero flux. This theory provides a novel way for exploring the global stability, function and the robustness of ecosystems.

Citation: Xu L, Zhang F, Zhang K, Wang E, Wang J (2014) The Potential and Flux Landscape Theory of Ecology. PLoS ONE 9(1): e86746. doi:10.1371/journal.pone.0086746

Editor: Antoni Margalida, University of Lleida, Spain

Received July 6, 2013; **Accepted** December 16, 2013; **Published** January 30, 2014

Funding: This study was supported by NSFC grant no. 21190040, 91227114, and 11174105; 973 project 2010CB933600; and NSF. The funders had no role in study design, data collection and analysis, decision to publish, or preparation of the manuscript.

Competing Interests: The authors have declared that no competing interests exist.

* E-mail: jin.wang.1@stonybrook.edu

☯ These authors contributed equally to this work.

Introduction

Ecosystems are the ones in which their living and nonliving components interact with and depend on each other linking together the exchange of energy, material, information. The structure and the function of the ecosystems are determined by the interplay of both cooperation and competition [1,2]. Ecosystems are able to regulate themselves to maintain certain stability. Therefore, the stability is one of the most fundamental and essential features of the ecological systems. The study of stability is direct relevant to the existence of every species. The stability is influenced by many factors, such as the structure within the components and the features of the environment. The studies of the stability of ecosystems are significant for uncovering the underly ecological law of species and populations [1,2].

The ecosystems are complex and involve many kinds of interactions among the elements. The inherent interactions are often non-linear and intricate. These systems can be described by a set of nonlinear differential equations [3,4]. These nonlinear interactions lead to complex dynamics. There have been many investigations on the stability of ecosystems [3–11]. Most of the works have been focused on the local linear stability analysis. The global stability of the ecological systems is still challenging in general. Furthermore, the link between the global characterization of the ecological systems and the dynamics of the elements is still not clear.

The past researchers also explored the dynamical system with the approach of Lyapunov function which was developed to investigate the global stability. The analytical Lyapunov function for predation model was first proposed by Volterra in 1931 [4]. Since then, significant efforts have been devoted to find the analytical Lyapunov function [5–8,10,11] for ecological equations. However, it is still challenging to find the Lyapunov function of the ecological models with the general nonlinear response terms, even though a few highly simplified ones were worked out [5,8]. So far there is no general and universal approach for finding the Lypunov function. One has to work case by case. There is even no guarantee if a Lyapunov function exists for a more complex system. Furthermore the Lyapunov function and the stability of a predation model with a solution of limit cycle have hardly been discussed. Here we would like to suggest an universal and straightforward approach to explore the Lyapunov function and therefore the global stability of the general ecological systems.

In the earlier studies, people have aimed at macroscopic properties based on the deterministic models. However, both external and intrinsic fluctuations of mesoscopic and even macro scale systems are unavoidable. The environmental fluctuations can influence the ecological behaviors. The intrinsic fluctuations emerge when the size of system is finite. It is widely agreed that the analysis of the global stability is important for a full understanding of the robustness of ecological systems under

fluctuations [5–7,11–13]. As mentioned, it is challenging to explore global stability with deterministic dynamics. The probability (P) description is necessary due to the presence of fluctuations of the real systems. The probability description has the advantage of quantifying the weights in the whole population state space and therefore is global. The potential landscape U linked with the probability P by $U \sim lnP$ can address global properties of ecosystems, such as the global stability, function and robustness.

Here we developed a potential and flux landscape theory to explore the global stability and dynamics for ecosystems [14–19]. We found that the underlying intrinsic potential landscape is a global universal Lyapunov function for the ecosystem dynamics and therefore topology of the landscape provides a quantitative measure for the global stability of the ecosystems. We also found the dynamics of the ecosystems is determined by the gradient of the potential landscape and additional curl flux force from breaking down of the detailed balance.

We applied our theory to three important ecosystems: predation, competition, mutualism and a realistic lynx-snowshoe hare model. Lotka-Volterra model for two species interactions is the famous ecological model proposed by Lotka [3]and Volterra [4] respectively. Over the years, this model has attracted attentions for exploring the dynamical process of the ecology. In the ecosystems, the relationship between species can be grouped into two categories: the negative antagonism interaction(−) and the positive mutualism interaction(+). We show the different modes in Figure 1. Predation shows the relationship (+/−) which one species S_A is disfavored, while the other species S_B benefits in Figure 1A; Competition shows the relationship(−/−) which each species S_A or S_B is influenced negatively by the other one in Figure 1B; Mutualism shows the relationship (+/+) which both species S_A and S_B benefit from interactions of the other in Figure 1C [2,6,11].

For the predation, predators sustain their lives by the consumption of preys. Without the presence of prey, predators can not survive. Preys can sustain their lives and grow without predators. The presence of the preys controls the predators' growth. This forms a predator-prey(predation) system [2–4]. The system can have one stable state or stable limit cycle. Competition between species often occurs when they are using the same resources. Competition can promote the ecological characteristics of species differentiation and produce certain biological structure of community. The system can have multi-stable states. Mutualism means that two different species biologically interact with each other and lead to benefit each individuals. The system can also have multi-stable states. These relations above demonstrate the complexity of biological communities,their stable structures, and the ecological balance [2,6,11]. These models are important for population biology because of its applications to the real biological world.

Limit cycle attractor shown in Figure 1D(Mexican hat shape)and multiple attractors shown in Figure 1E emerge from these three cases: predation, competition and mutualism. Figure 1D and Figure 1E show the potential landscapes closely associated with the probability distribution for the underlying ecosystem. The lower potential landscape means the higher probability and therefore more stable states. The closed ring valley is a continuous attractor for oscillation while the discrete basins represent the stable attractors on the potential landscapes. We found the quantitative criterion for stability in terms of barrier height between basins of attraction. The barrier height from the top of the Mexican hat to the ring valley of limit cycle attractor (the potential maximum along the limit cycle) in Figure 1D or between each two attractors(from the saddle point to the minimum of each basin) in Figure 1E quantitatively determine the global stability of these ecosystems. The curl flux is essential for driving the oscillation on the valley ring and maintaining the coherence. We studied stability and robustness of ecosystems against parameters and fluctuations. We also explored how the non-equilibrium free energy links with the different phases and phase transitions of the ecosystem with respect to the changes of parameters. These explained how the stability and robustness of ecosystem change under different conditions. Quantification of pathway is important for understanding the dynamics of ecosystem. We developed the path integral method to quantify the kinetic pathway of ecosystems. We found that the paths do not

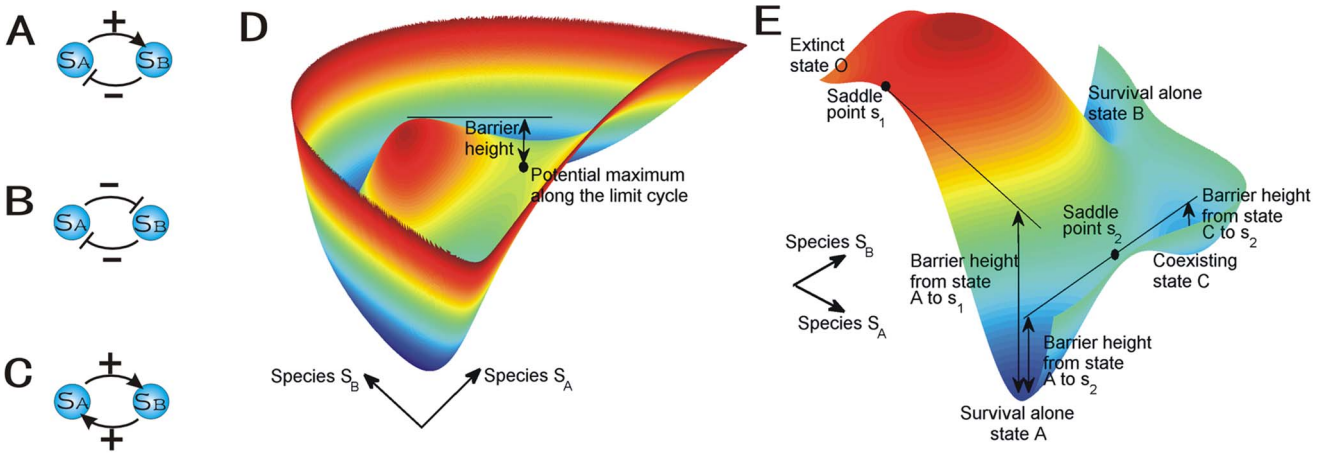

Figure 1. The schematic diagram for the ecological models. (A)Predation model. (B)Competition model. (C)Mutualism model. The potential landscape U is linked with the probability P by $U \sim lnP$ in species space. (D) Limit cycle attractor. The barrier height from the maximum inside the closed ring to the potential maximum along the ring can quantify the stability of the limit cycle attractor. (E) Multiple attractors. There are four stable states: survival alone state A of species S_A, survival alone state B of species S_B, coexisting state C, and both extinct state O. s_1 is the saddle points between the attractors A and O while s_2 is the saddle points between the attractors A and C. The barrier heights from the saddle points to the potential minimums of the basins can quantify the stability of each attractor.
doi:10.1371/journal.pone.0086746.g001

follow gradient of the underlying potential landscape and are irreversible because of the non-zero flux.

Results and Discussion

The potential landscapes and fluxes of ecosystems: predation, competition and mutualism

We quantified the underlying potential landscape of the ecosystems through the exploration of the underlying dynamics of probability. We solved the Fokker-Planck diffusion equation describing the probability dynamics to obtain the population potential landscape U related to the steady state probability distribution P_{ss} through $-lnP_{ss}$ and steady state probability flux $\mathbf{J}$. We explored the Hamilton-Jacobi equation in zero noise limit to quantify the intrinsic potential landscape ϕ_0 with Lyapunov properties and the associated intrinsic flux velocity. The details are in the Materials and Methods section. We will discuss how to apply the landscape theory of intrinsic potential landscape ϕ_0, the population potential landscape U and the probability flux $\mathbf{J}$ to explore the global stability and dynamics of the three ecosystem models.

The population potential landscape U (the top row) and intrinsic potential landscape ϕ_0 (the bottom row)for predation, competition and mutualism model are shown respectively in Figure 2. The negative gradient of the population potential landscape $-\nabla U$ on the top row and the intrinsic potential landscape $-\nabla\phi_0$ on bottom row are represented by the black arrows while the steady state probability flux $\mathbf{J}_{ss}/P_{ss}$ on the top row and the intrinsic flux velocity on the bottom row are represented by the purple arrows. The arrows at the bottom of each sub-figures are the projection of the direction of the according arrows. The flux with purple arrows are almost orthogonal to the negative gradient of U with black arrows shown on the bottom plane of Figure 2A, Figure 2B and Figure 2C. The flux velocity with purple arrows are orthogonal to the negative gradient of ϕ_0 with black arrows shown on the bottom plane of Figure 2D, Figure 2E and Figure 2F.

Figure 2A and Figure 2D show the non-equilibrium population potential landscape U and intrinsic potential landscape ϕ_0 for predation model when the parameters are $a=1.5$, $b=0.1$, $d=0.2$, $D=3\times10^{-5}$. The mathematical model and the range of the parameters are discussed in Materials and Methods section. We can see when the fluctuations characterized by the diffusion coefficient are small, the underlying potential landscape has a distinct closed irregular and inhomogeneous closed ring valley or Mexican hat like shape shown in Figure 2A. We can clearly see the population potential landscape is not uniformly distributed along the limit cycle path or the closed ring. The intrinsic potential landscape ϕ_0 has a homogeneous closed ring valley along deterministic oscillation trajectories which has a constant value of ϕ_0 shown in Figure 2D. The non-equilibrium intrinsic potential landscape ϕ_0 with Lyapunov properties can characterize the global topography of the oscillation landscape of predation model. This figure shows the potential is lower along the oscillation path or on the ring. The potential landscape is higher with a mountain inside the oscillation ring and outside the oscillation ring. The system is attracted to the closed oscillation ring by the landscape's gradient-potential force ∇U or the $\nabla\phi_0$. The flux driving the system maintains the periodical continuous oscillation dynamics. Both landscape and flux are necessary to characterize the non-equilibrium predation ecosystems. This oscillation shows that when the number of predators increases, more preys will be consumed. Then due to the shortage of food, the number of the predator will go down. The reduction of the predators makes the preys multiply, then the number of predators increases again for the rich preys.

Figure 2B and Figure 2E show the non-equilibrium population potential landscape U and intrinsic potential landscape ϕ_0 for competitive model when the parameters are $a_1=a_2=0.1$, $L_1=L_2=0.3$, $\alpha=1.0$, $D=0.01$. We can see the underlying population potential landscape and intrinsic potential landscape both have four distinct basins which have been discussed in the Materials and Methods section. The basins are around the four stable states. These four stable states are: survival alone state A of species S_A, survival alone state B of species S_B, coexisting state C, and both extinct state O. These figures show the potential landscape is relatively higher (and probability is relative lower) on the extinct state (the state O) of these two species because the lower critical points L_1,L_2 for species are small. The potential landscapes of the survival alone state A and B are lower(more stable) than that of the coexisting state C. It shows that the coexisting state is less stable than the species survival alone states for they have competitive relation. The forces from negative gradient of the potential landscape are more significant away from the attractors and less significant near the basins. Therefore the system is attracted by the gradient of the landscape towards the four basins. The directions of the flux are curling among the basins.

Figure 2C and Figure 2F show the non-equilibrium population potential landscape U and intrinsic potential landscape ϕ_0 for mutualism model when the parameters are $a_1=a_2=0.1$, $L_1=L_2=0.5$, $\alpha=1.0$, $D=0.01$. The underlying population potential landscape and intrinsic potential landscape both have distinct four basins. The basins are around the four stable states. These figures show the potential landscape is the highest (and probability is lower) on the extinct state O of these two species. The potential landscape of mutualism coexisting state C is lowest than those of species survival alone state A and B, and the extinct state O. It shows that the coexisting state is more stable than the species alone state for the two species having the relationship of mutualism. The directions of the flux are curling among the four basins. And the system is also attracted by the gradient of landscape towards the four basins.

Quantitative measure of global stability for predation

We now study the stability and robustness of the ecosystems. The stability is related to the escape time from the basins. Since the system is characterized by the basins of attractor with large weights, the easier it is to escape, the less stable the system is. We will essentially explore the average time escaping from a basin of attraction.

We define the barrier height of U for predation model as: $Ba=U_{fix}-U_{max}$. U_{max} is the population potential maximum along the limit cycle attractor. U_{fix} is the population potential landscape at the local maximum point inside the limit cycle. And the barrier height of ϕ_0 for predation model is defined as: $\Delta\phi_0=\phi_{0fix}-\phi_{0max}$. ϕ_{0max} is the intrinsic potential maximum along the limit cycle attractor. ϕ_{0fix} is the intrinsic potential landscape at the local maximum point inside the limit cycle. The escape time τ can be solved by the formula [20]: $\mathbf{F}\cdot\nabla\tau+D\cdot\nabla^2\tau=-1$. It represents the average time the system spent from one position to another position [18].

We showed the change of population potential landscapes for increasing diffusion coefficient D (Figure S1 in File S1). In Figure 3A, the barrier heights associated with escape time from the limit cycle attractor Ba becomes higher when the diffusion coefficient characterizing the fluctuations decreases. In Figure 3B, we see a direct relationship between the escape time τ from the

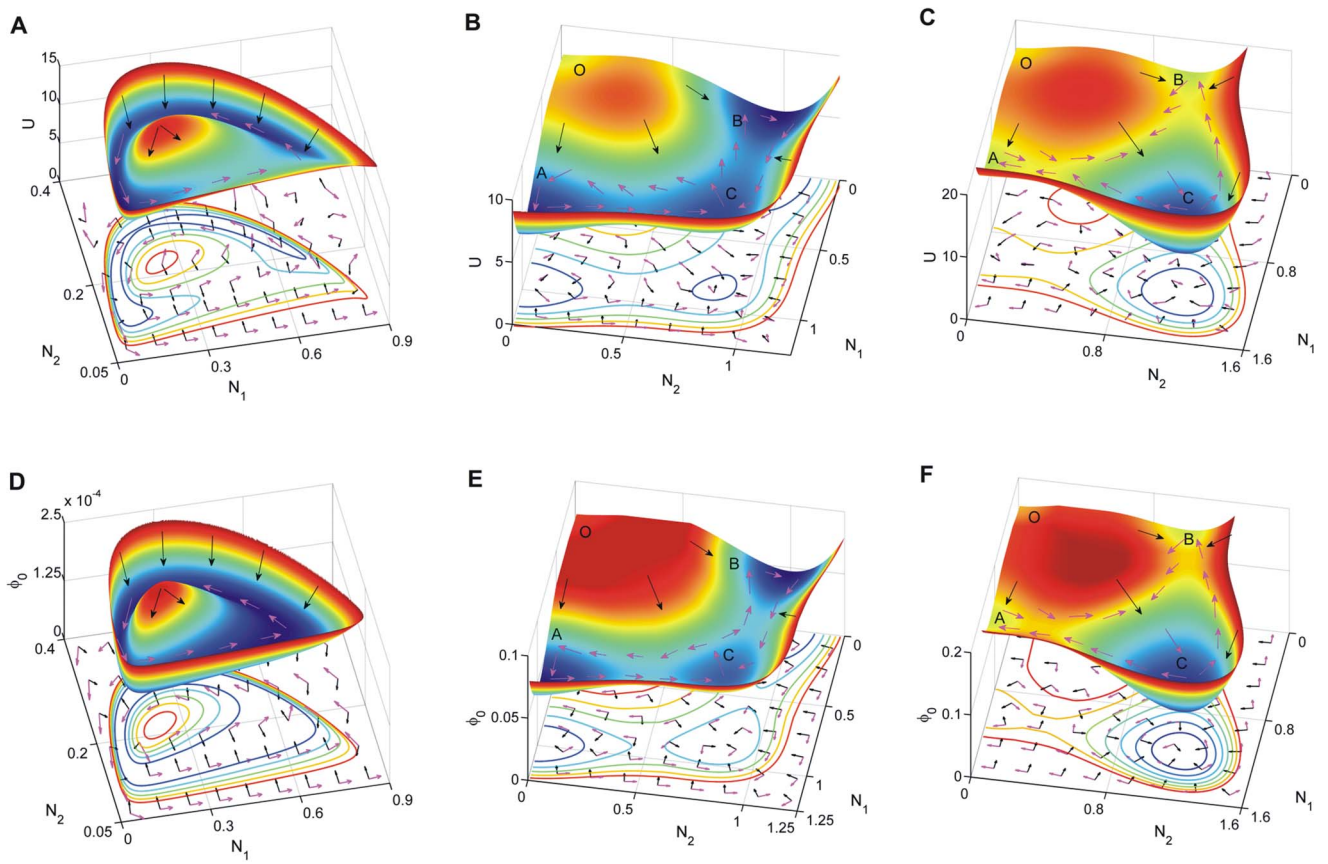

Figure 2. The potential landscapes for the predation, competition and mutualism models. Top row: The population potential landscape U ((A) predation model. (B) competition model. (C) mutualism model.) Purple arrows represent the flux velocity($\mathbf{J}_{ss}/P_{ss}$) while the black arrows represent the negative gradient of population potential($-\nabla U$). Bottom row: The potential intrinsic energy landscape ϕ_0. ((D) predation model. (E) competition model. (F) mutualism model.). Purple arrows represent the intrinsic flux velocity($\mathbf{V}=(\mathbf{J}_{ss}/P_{ss})_{D\to 0}$) while the black arrows represent the negative gradient of intrinsic potential($-\nabla\phi_0$).
doi:10.1371/journal.pone.0086746.g002

limit cycle attractor [17,18] and barrier height for non-equilibrium ecosystems. As the barrier height for escape becomes higher, the escape time becomes longer. Therefore, the limit cycle attractor becomes more stable since it is harder to go from the valley ring to outside. The robustness and stability in the oscillatory predation system need small fluctuations and large barrier height. Figure 3C shows the heat dissipation rate $HDR=\int(\mathbf{J}\cdot(\mathbf{F}-\nabla\cdot\mathbf{D}))d\mathbf{N}=\int\mathbf{J}\cdot\mathbf{F}d\mathbf{N}$ (see the Materials and Methods section 1 for details)versus different diffusion coefficients. We can see the heat dissipation rate decreases when the diffusion coefficient decreases. This implies that when the fluctuations deduce, the associated heat dissipation rate becomes smaller. We have explored that less fluctuations lead to more robust and stable oscillation with higher barrier height. Therefore, the less dissipation can lead to less fluctuations and a more stable ecosystem with longer escape time.

We also explored the effects of the rate parameters representing interaction strengths between species on the robustness. We showed the change of population potential landscapes for increasing parameters a,b,d (Figure S2 in File S1, Figure S3 in File S1 and Figure S4 in File S1). We show the effects of rate parameters a,b,d on the robustness through barrier height in Figure 4A, Figure 4D and Figure 4G; the escape time τ in Figure 4B, Figure 4E and Figure 4H; the dissipation rate in Figure 4C, Figure 4F and Figure 4I with $D=3\times10^{-5}$. For the small parameter a, the relative death rate or the interaction strength for the prey is very small, the prey and the predator both are near their carrying capacities. The stable point is $N_1^*=N_2^*$, where the population of the predator is equal to the population of the prey. The system is attracted to its stable coexisting state. When the relative death rate or the interaction strength increases to a certain specific range, the system can reach a limit cycle state since it is a negative feedback system. When the parameter a continues to increase beyond the range of limit cycle, the death rate or the interaction strength of the preys increases, the preys decrease. The lack of food leads to the reduction of the predators. So the system reaches a stable state that both predator and preys have low population. The Ba versus a increases first, then decreases as shown in Figure 4A. Figure 5A shows barrier height $\Delta\phi_0$ of the intrinsic potential landscape(ϕ_0) has the same tendency with that of the population landscape. It implies the system first becomes more stable, and then less stable when the parameter a increases in the range of limit cycle. The system has an optimal stability in this range. This is due to the fact that both decreasing and increasing a from optimal stability of the limit cycle will promote the formation of mono-stability and make the limit cycle less stable. Figure 4B shows the average escape time versus the barrier height Ba. When the barrier height for escape becomes higher, the escape time becomes longer. Figure 4C shows the dissipation rate increases with the increasing parameter a. It implies that the system will consume more energy to keep order

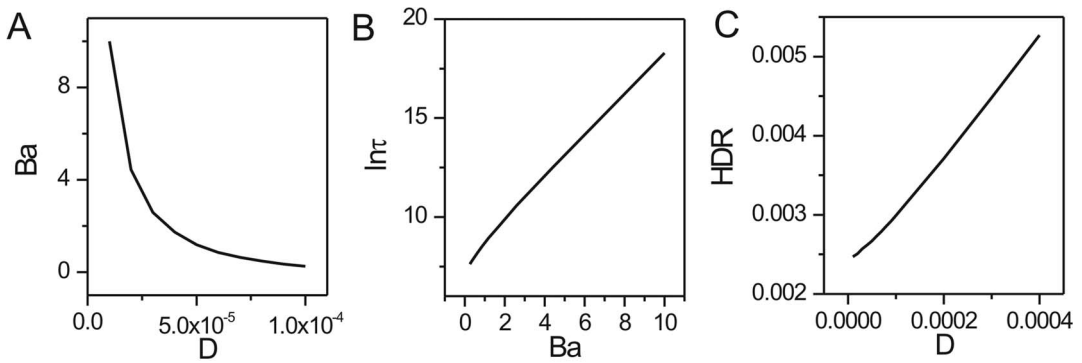

Figure 3. The barrier height of population landscape, escape time and dissipation rate versus the diffusion coefficient for predation model. (A) The barrier height of the population landscape U versus the diffusion coefficient D. (B) The escape time versus the barrier height of population landscape. (C) The dissipation rate versus the diffusion coefficient D.
doi:10.1371/journal.pone.0086746.g003

when the system stays at limit cycle oscillation state than when it stays at one stable state with the transition point $a=1.109$. Figure 5D shows the intrinsic free energy(see the Materials and Methods section 2 for details) versus a. We can see clearly the non-equilibrium free energy is continuous versus parameter a, the first derivative of the free energy is discontinuous at the transition point $a=1.109$ from a stable state to a limit cycle oscillation state. It is a signal of non-equilibrium thermodynamic phase transition analogous to equilibrium statistical mechanics. The non-equilibrium free energy for ecosystem can measure and predict the global phases transitions and can be use to investigate the global natural stability and robustness of the ecosystem.

When the parameter b which represents the ratio of the linear growth rate of the predator to that of the prey is small, the system stays at the specific range of limit cycle state. When the parameter b continues to increase, the growth rate of the predator increases, so the prey decreases and therefore it will lead the predator to decrease. So the system will stay at a stable state where the predator and prey both keep relative lower population. The Ba versus b decreases shown in Figure 4D. Figure 5B shows barrier height of the intrinsic potential landscape(ϕ_0) has the same tendency with the population potential landscape. This implies that the limit cycle attractor becomes less stable when the ratio of the linear growth rate of the predator increases. Figure 4E shows the average escape time versus the increasing parameter b has the same tendency with the barrier height versus the increasing parameter b. Figure 4F shows that the dissipation rate decreases with the increasing parameter b. Figure 5E shows the free energy versus b. The first derivative of the non-equilibrium free energy is discontinuous at the transition point $b=0.1899$ from a limit cycle oscillation state to a stable state.

The predation term $\frac{aN_1N_2}{N_1+d}$ which is the response of the predator to the change in the prey density, shows the saturation effect. When the parameter d which represents the relative saturation effect rate of the prey is small, the system stays at the specific range of the limit cycle state as saturation point of predation is very low. When the parameter d continues to increase, the response term and the death rate of the preys decreases, so the preys and the predators are in a relative lower population stable state. The barrier height Ba decreases as d increasing shown in Figure 4G. Figure 5C shows barrier height of the intrinsic potential landscape(ϕ_0) has the same tendency with the population landscape. This implies that the limit cycle attractor of this system becomes less stable when the saturation point of predation increasing. Figure 4H shows the average escape time versus the increasing parameter d has the same tendency with the Ba versus the increasing parameter d. Figure 4I shows that the dissipation rate decreases with the increasing parameter d. The system becomes less stable. Figure 5F shows the free energy versus d. The transition point $d=0.2715$ shows the system transits from a limit oscillation state to a stable state.

We also can use the phase coherence to quantify the robustness and the stability of a cycle [17,18,21]. Coherence ζ represents the degree of the regularity in time sequence of cycle motion of species variables in the ecosystem. The vector $M(t)=n_1(t)e_1+n_2(t)e_2$ is set with $e_1=(0,1)$ and $e_2=(1,0)$ as the unit vectors, as well as n_1 and n_2 represent the population of each species at time t. $w(t)$ is the phase angle between $M(t)$ and $M(t+\tau)$. Then the ζ is defined as $\zeta=(2\sum_i \theta(w(t_i))w(t_i))/(\sum_i |w(t_i)|)-1$ [17,18,21]. ($\theta=1$ if $w>0$, and $\theta=0$ if $w\leq 0$) The larger value of coherence close to 1 means the more periodic while the smaller value of coherence close to 0 means the less periodic. In Figure 6A, ζ decreases when the diffusion coefficient increases. This means larger fluctuations will reduce the coherence and the robustness of the oscillations.Figure 6B, Figure 6C and Figure 6D show the ζ versus the parameter a,b,d. We found that they have nearly the same tendency with the barrier height versus the parameters a,b,d shown in Figure 4A, Figure 4D and Figure 4G. It implies that the higher barrier height lead the system to have more coherent periodic oscillation, and therefore the system is more stable.

Quantifying the global stability of competition ecosystems

For competition and mutualism models, we introduced the effective barrier heights for simplicity. The effective barrier heights are similar to the effective resistance of parallel circuits. They can measure the effect of average barrier on a single basin. We defined the effective barrier heights for state i in population potential U as: $Ba_i=\frac{(Us_{ij}-U_i)*(Us_{ik}-U_i)}{(Us_{ij}-U_i)+(Us_{ik}-U_i)}$ where $\{i,j,k\}\in\{\{A,O,C\},\{B,O,C\},\{C,A,B\}\}$. When the system has four stable states: survival alone state A of species S_A, survival alone state B of species S_B, coexisting state C, and both extinct state O. Us_{ij} is the population landscape value of saddle point between state i and state j. U_A, U_B, U_C and U_O are the values of population landscape at state A, B, C and O. When the coexisting state C vanishes, we defined the $Ba_i=\frac{(Us_{ij}-U_i)*(Us_{ik}-U_i)}{(Us_{ij}-U_i)+(Us_{ik}-U_i)}$ where $\{i,j,k\}\in$

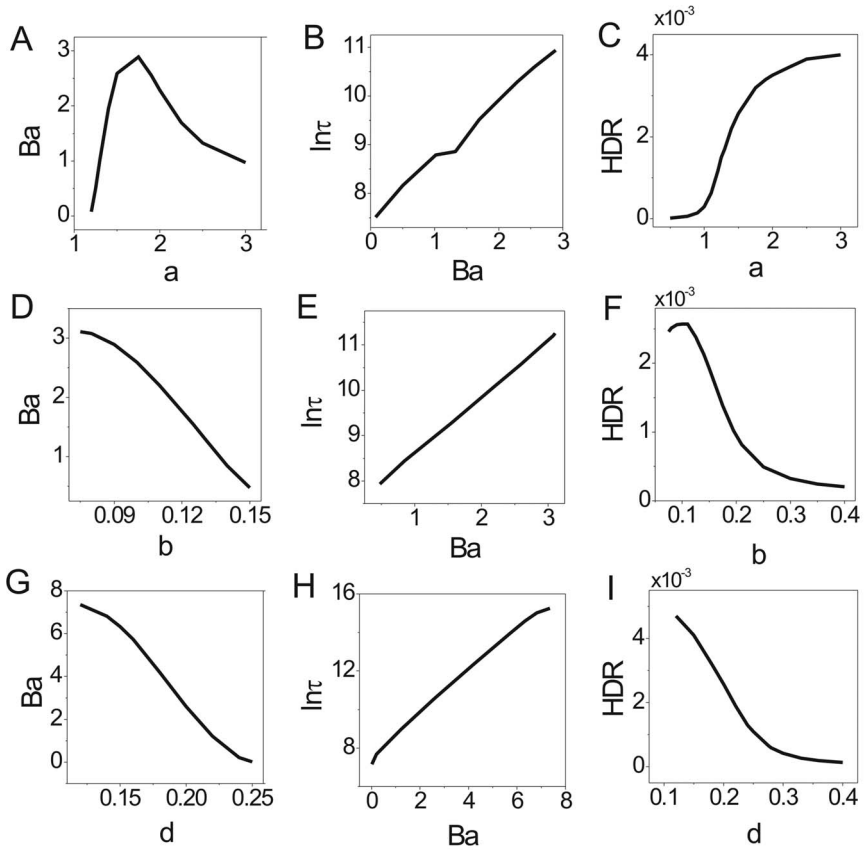

Figure 4. The barrier height of the population landscape, escape time and dissipation rate versus the rate parameters for predation model. (A) The barrier height of the population landscape versus a. (B) The escape time versus barrier height of the population landscape for changing a. (C) The dissipation rate versus a. (D) The barrier height of the population landscape versus b. (E) The escape time versus barrier height of the population landscape for changing b. (F) The dissipation rate versus b. (G) The barrier height of the population landscape versus d. (H) The escape time versus barrier height of the population landscape for changing d. (I) The dissipation rate versus d.
doi:10.1371/journal.pone.0086746.g004

$\{\{A,O,B\},\{B,O,A\}\}$, We also defined the effective barrier heights in intrinsic potential as: $\Delta\phi_{0i}=\frac{(\phi_{0ij}-\phi_{0i})*(\phi_{0ik}-\phi_{0i})}{(\phi_{0ij}-\phi_{0i})+(\phi_{0ik}-\phi_{0i})}$ where $\{i,j,k\}\in\{\{A,O,C\},\{B,O,C\},\{C,A,B\}\}$ when the system has four stable states A,B,C,O. When the coexisting state C vanishes, we defined the $\Delta\phi_{0i}=\frac{(\phi_{0ij}-\phi_{0i})*(\phi_{0ik}-\phi_{0i})}{(\phi_{0ij}-\phi_{0i})+(\phi_{0ik}-\phi_{0i})}$ where $\{i,j,k\}\in\{\{A,O,B\},\{B,O,A\}\}$. ϕ_{0ij} is the intrinsic landscape value of saddle point between state i and state j. ϕ_{0A}, ϕ_{0B}, ϕ_{0C} and ϕ_{0O} are the intrinsic potential landscape values of state A, B, C and O.

We showed the change of population potential landscapes for increasing diffusion coefficient D (Figure S5 in File S1). Figure 7 shows diffusion effect on the competition model. In Figure 7A, as the diffusion coefficient characterizing the fluctuations decreases, the barrier heights $Ba_{A(B)}$ and Ba_C are higher when the parameters are $a_1=a_2=0.1, L_1=L_2=0.3, \alpha=1.0$. Figure 7B shows the escape time versus the barrier height Ba_A. We can see the system is harder to escape from the basins of attraction as the fluctuation decreases, and the barrier height also increases. Figure 7C shows the dissipation rate for different diffusion coefficients. We can see the heat dissipation rate decreases when the diffusion coefficient decreases and the fluctuations of the systems become smaller.

We showed the change of population potential landscapes for increasing parameters a_1, L_1, α (Figure S6 in File S1, Figure S7 in File S1 and Figure S8 in File S1). Figure 8A, Figure 8B and Figure 8C show the effects of rate parameter a_1 on this system at $D=0.001$. When a_1, the competitiveness of S_B on S_A decreases, the competitiveness of species S_B becomes weaker while that of species S_A becomes stronger, so the barrier height Ba_A increases while Ba_B decreases. With the parameter (a_1) further weakened the competitiveness of the species S_B, the two species can achieve their coexisting state C. The coexisting state C becomes more stable as the competitiveness of B on A decreases shown in Figure 8A. Figure 9A shows barrier height of the intrinsic potential landscape(ϕ_0) has the same tendency with that of the population landscape. This implies the two species can coexist stably as the mutual competitiveness is reduced. The logarithm of escape time $ln\tau_A$ from basin A has positive correlation with barrier height Ba_A shown in Figure 8B. The escape time increases when the associated barrier height becomes higher.

Figure 8D, Figure 8E and Figure 8F show the effects of rate parameter L_1 on competition system with $D=0.001$. When L_1 increases, the lower critical number or density of species S_A becomes larger, so the survival alone state A of species S_A becomes less stable and shallower while the other survival alone state B becomes more stable and deeper (The barrier height Ba_B increases,Ba_A and Ba_C decrease as L_1 increases shown in Figure 8D. The escape time $ln\tau_A$ from basin A has positive correlation with Ba_A shown in Figure 8E. Figure 9B shows barrier height of the intrinsic potential landscape(ϕ_0) has the same

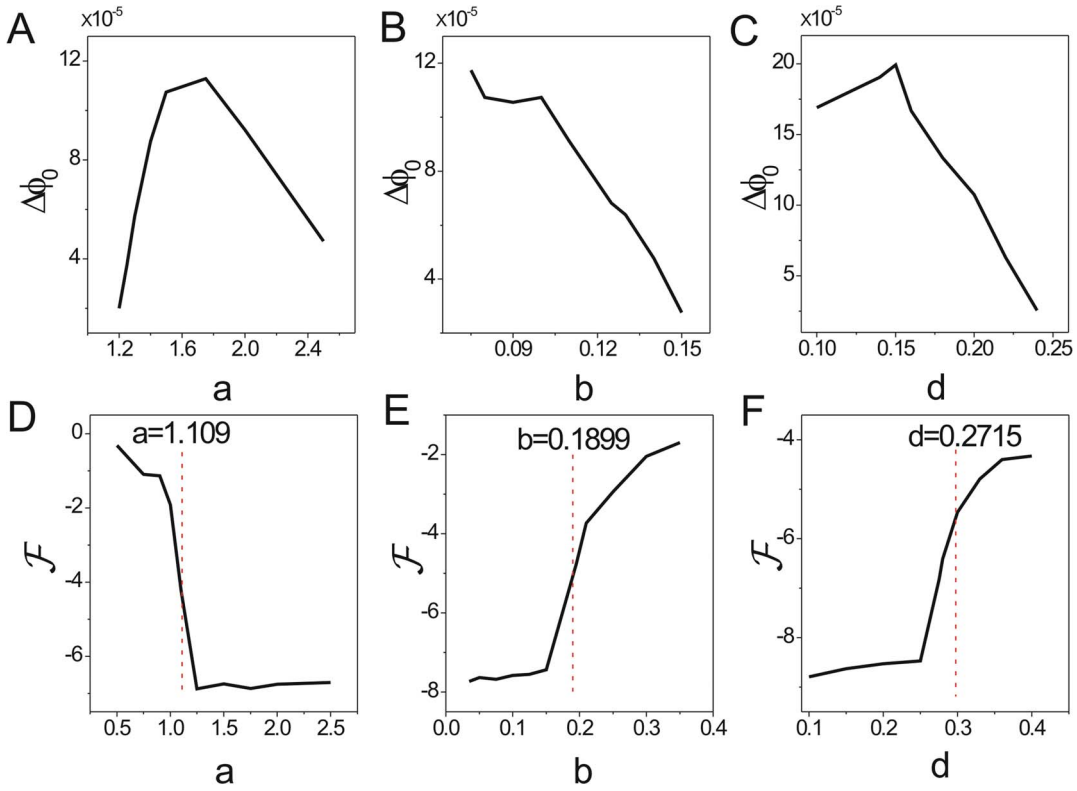

Figure 5. The barrier height of intrinsic potential landscape and free energy versus the rate parameters for predation model. The barrier heights of intrinsic potential landscape versus parameters a (A), b (B), d (C). The free energy versus a (D), b (E), d (F).
doi:10.1371/journal.pone.0086746.g005

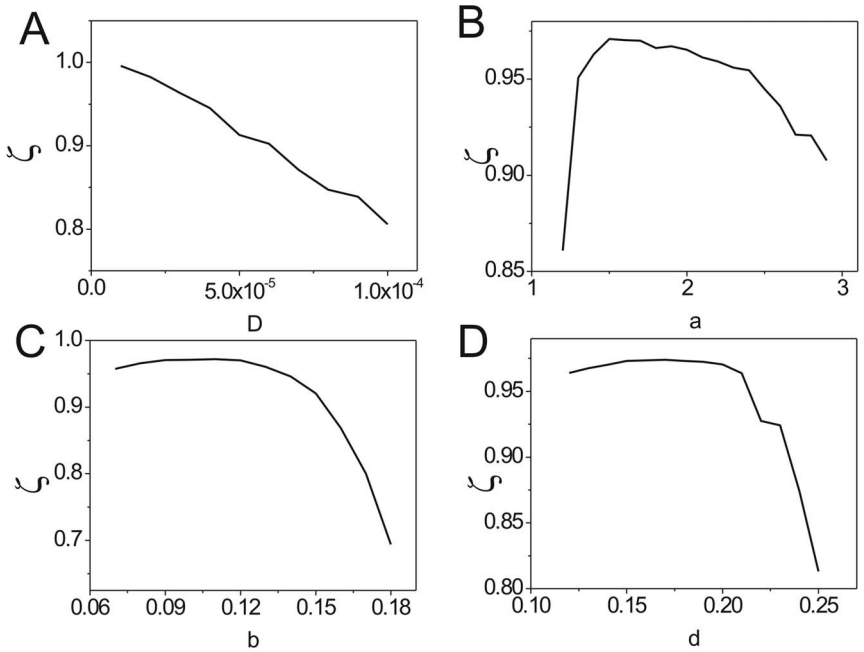

Figure 6. The coherence for predation model. (A)The coherence versus the diffusion coefficient. (B) The coherence versus the parameter a. (C) The coherence versus the the parameter b. (D) The coherence versus the the parameter d.
doi:10.1371/journal.pone.0086746.g006

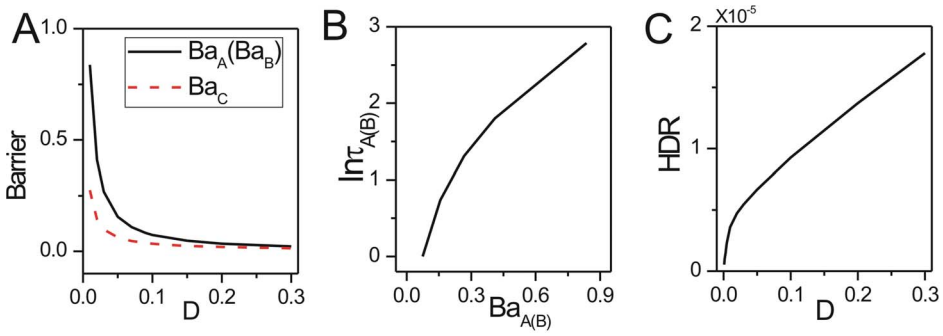

Figure 7. The barrier height of the population landscape, escape time and dissipation rate versus the diffusion coefficient for competition model. (A) The barrier height of the population landscape U versus the diffusion coefficient D. (B) The escape time versus the barrier height of the population landscape. (C) The dissipation rate versus the diffusion coefficient D.
doi:10.1371/journal.pone.0086746.g007

tendency at those of the population landscape.), and the coexisting state C generally vanishes(The barrier height Ba_C decreases). It implies that when the lower critical number or density of species S_A becomes larger, the species S_A will extinct easily. The competitiveness for species S_B becomes larger, so it will live more stably.

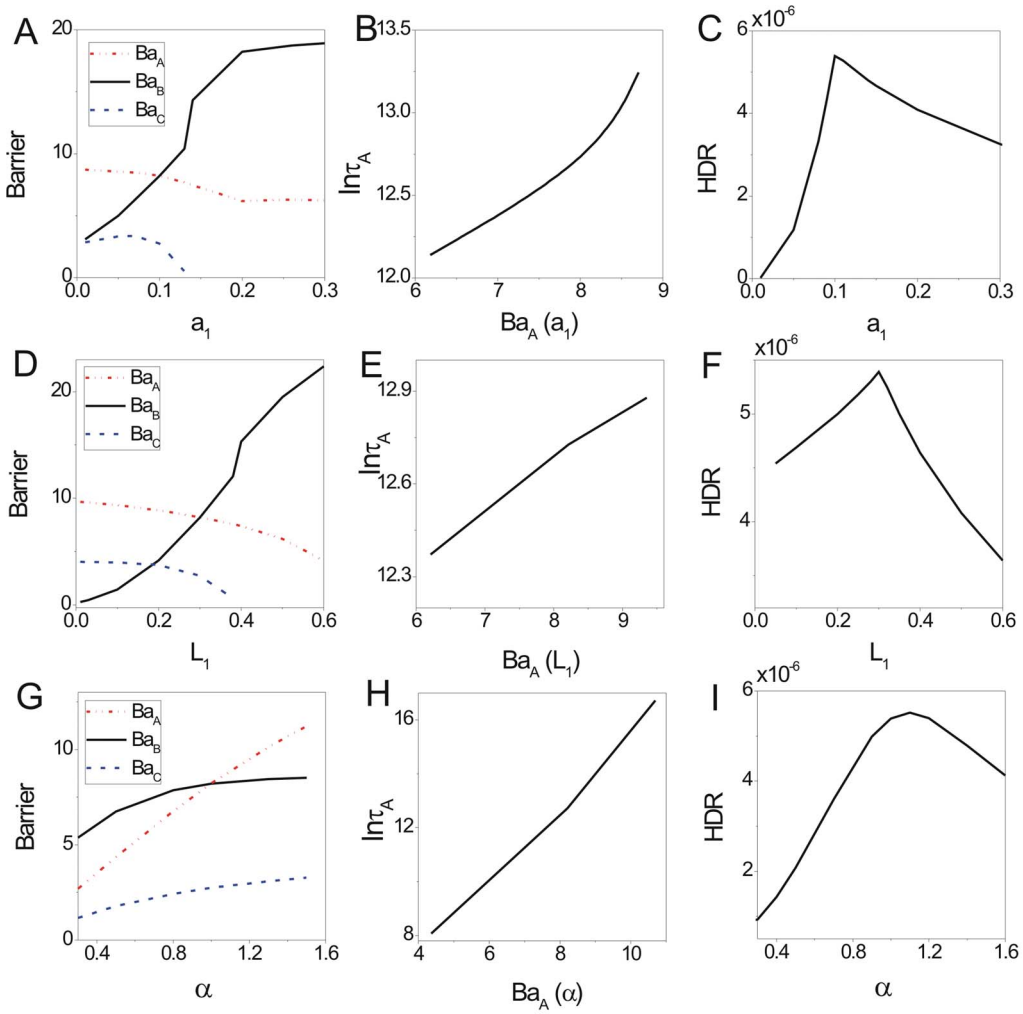

Figure 8. The barrier height of the population landscape, escape time and dissipation rate versus the rate parameters for competition model. (A) The barrier height of the population landscape versus a_1. (B) The escape time versus barrier height of the population potential landscape. (C) The dissipation rate versus a_1. (D) The barrier height of the population potential landscape versus L_1. (E) The escape time versus barrier height of the population potential landscape. (F) The dissipation rate versus L_1. (G) The barrier heights of the population landscape versus α. (H) The escape time versus barrier height of the population potential landscape. (I) The dissipation rate versus α.
doi:10.1371/journal.pone.0086746.g008

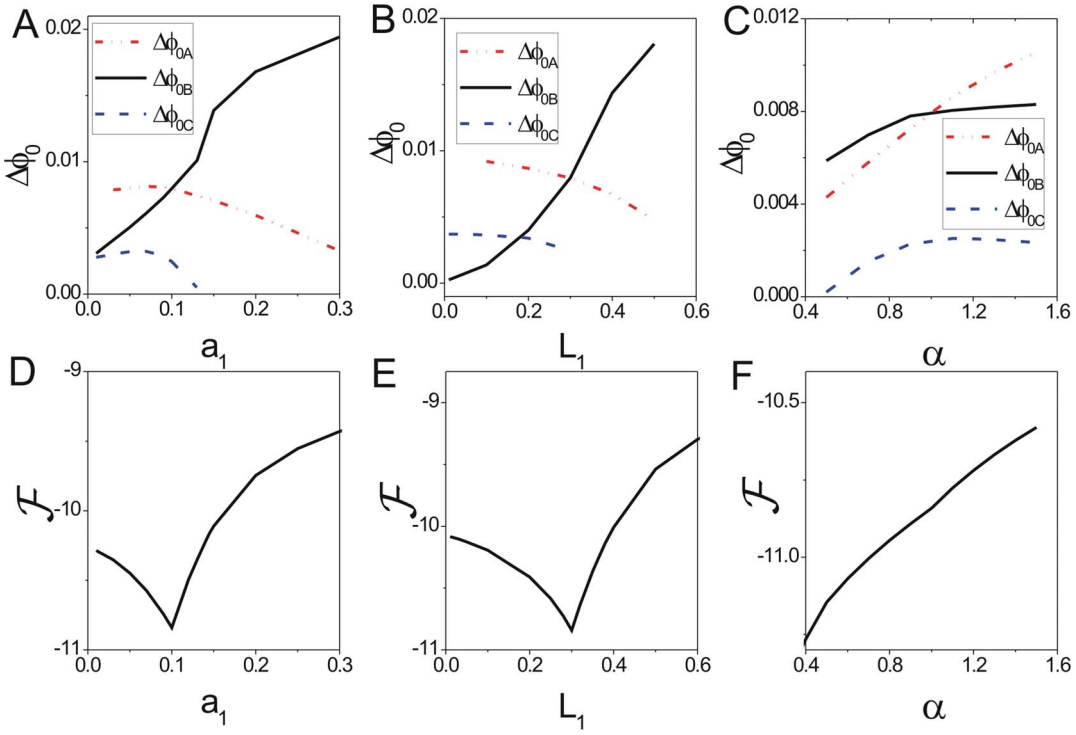

Figure 9. The barrier height of intrinsic potential landscape and free energy versus the rate parameters for competition model. The barrier heights of intrinsic potential landscape versus a_1 (A), L_1 (B), α (C). The free energy versus a_1 (D), L_1 (E), α (F).
doi:10.1371/journal.pone.0086746.g009

Figure 8G, Figure 8H and Figure 8I show the effects of rate parameter α which means the relative birth rate of species S_B on this system with $D=0.001$. When α increases, the relative birth rate of species S_B becomes larger, so the survival alone basin B of species S_B becomes more stable and deeper. The other survival alone state A and the coexisting state C also become more stable and deeper (The barrier height Ba_A increases shown in Figure 8G and the escape time $ln\tau_A$ becomes longer shown in Figure 8H. They are positively correlated.Figure 9C shows the barrier height of the intrinsic potential landscape(ϕ_0) has the same tendency with that of the population landscape.) It implies that when the birth rate of B becomes larger, the species S_B will be more stable. This can lead the coexisting state C and the survival alone state A to become more stable.

Figure 8C, Figure 8F and Figure 8I show the heat dissipation rates increase then decrease when the parameter a_1,L_1,α increase. The flux makes a significant contribution to the heat dissipation rate $HDR=\int \mathbf{J}\cdot\mathbf{F}d\mathbf{N}=\int \mathbf{J}\cdot(\mathbf{J}/P+D\nabla U)d\mathbf{N}$. The contribution of the term $D\nabla U$ is numerically much smaller than that of term $\mathbf{J}/P$ because the values of $D\nabla U$ are small in less fluctuations and their directions are near orthogonality to the flux. When the parameters are given specific values: $a_1=a_2=0.1$, $L_1=L_2=0.3$, $\alpha=1.0$, the system stays at a symmetrical landscape topography, so the depths of the basin A and basin B have the same value. These two basins both have large areas of dominant flux. As the three parameters increase or decrease, the system becomes less symmetrical in landscape topography, one area of the basin A or B becomes more dominant. Since the area of the dominant flux becomes less, the heat dissipation rate becomes less and the system consume less energy. Figure 9D shows the phase transition from four stable states to three stable states nearby $a_1=0.1$. The first derivative of the non-equilibrium free energy is discontinuous at this point, which is a signal of thermodynamic phase transition. Figure 9E shows the phase transition from four stable states to three stable states nearby $L_1=0.3$. Figure 9F shows the free energy increases as α increases, and has no phase transition.

Due to competitive exclusion principle, the two species competing for the same resources are impossible to coexist in the same area. So we can see the landscape for larger $a_1(a_2)$ can not have the coexisting state, but it can have two stable states for living alone. The system will eventually select one stable state according to the initial condition (the slightest advantage for one species)and the fluctuations in the environment. If they coexist in the same area, there must have differences on the ecological factors, such as habitat, diet, activity time or other characteristics among the competitive species.

Quantifying the global stability of the mutualism ecosystems

We showed the change of population potential landscapes for increasing diffusion coefficient D (Figure S9 in File S1). Figure 10 shows diffusion effect on the mutualism model. In Figure 10A, as the diffusion coefficient characterizing the fluctuations decreases, the barrier heights $Ba_{A(B)}$ and Ba_C becomes higher when the parameters are $a_1=a_2=0.1$, $L_1=L_2=0.5$, $\alpha=1.0$. Figure 10B shows the escape time versus the barrier height Ba_A. We can see clearly that the higher the barrier height is, the longer the escape time is. The system is harder to escape from the basins of attraction as the barrier height increases. Figure 10C shows the heat dissipation rate for different diffusion coefficients. We can see the dissipation or the entropy production rate decreases when the diffusion coefficient decreases.

We showed the change of population potential landscapes for increasing parameters a_1,L_1,α (Figure S10 in File S1, Figure S11

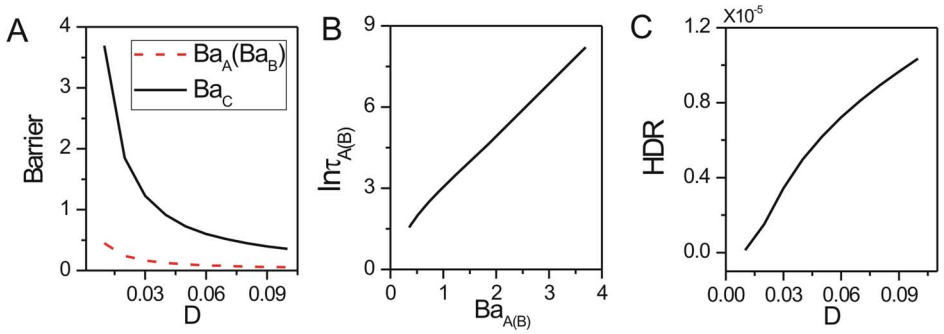

Figure 10. The barrier height of the population landscape, escape time and dissipation rate versus the diffusion coefficient for mutualism model. (A) The barrier height of the population landscape U versus the diffusion coefficient D. (B) The escape time versus the barrier height of the population landscape. (C) The dissipation rate versus the diffusion coefficient D.
doi:10.1371/journal.pone.0086746.g010

in File S1 and Figure S12 in File S1). Figure 11A, Figure 11B and Figure 11C show the effects of rate parameter a_1 on mutualism system at $D=0.002$. We can see when the value of a_1, the mutualism ability is small, there are four stable states. Here we also included the lower critical number or density, so the system can go to their mutual extinction state. The coexisting state C is deeper than the other two states A and B which represent the species living alone shown in Figure 11A. Figure 12A shows that the barrier height of the intrinsic potential landscape(ϕ_0) has the same tendency with that of the population landscape. This implies an obvious rule, mutual benefit can help the species to live and reproduce. As a_1 increases, the cooperative effect on species S_A becomes stronger, the coexisting state C become more stable and the escape time $ln\tau_C$ becomes longer as the barrier height Ba_C increases shown in Figure 11B. It implies that when the cooperative effect increases, the system will go to the coexisting stable state. With the increasing of the cooperative effect, the species can coexist in larger population than their respective carrying capacity.

Figure 11D, Figure 11E and Figure 11F show the effects of rate parameter L_1 on mutualism system with $D=0.002$. When L_1 increases, the lower critical number or density of species S_A becomes larger, so the survival alone basin A of species S_A becomes less stable and shallower while the other survival alone state B becomes more stable and deeper (The barrier height Ba_B increases, Ba_A and Ba_C decrease as L_1 increases shown in Figure 11D. The escape time $ln\tau_C$ from basin C has positive correlation with Ba_C shown in Figure 11E.) When the lower critical number of species S_A becomes larger further, the species S_A will become extinct easily. Figure 12B shows barrier height of the intrinsic potential landscape(ϕ_0) has the same tendency with that of the population landscape.

Figure 11G, Figure 11H and Figure 11I show the effects of rate parameter α which means the relative birth rate of species S_B on mutualism system with $D=0.002$. When α increases, the relative birth rate of species S_B becomes larger, so the survival alone basin B of species S_B becomes more stable and deeper (The barrier height Ba_B increases slightly.) The other survival alone state A and the coexisting state C also becomes more stable and deeper shown in Figure 11G. The escape time $ln\tau_C$ becomes longer according to the tendency of Ba_C shown in Figure 11H. It implies a rule that the increase in population growth of species S_A can lead to the result of greater number of species S_B, and vice versa. Figure 12C shows the barrier height of the intrinsic potential landscape(ϕ_0) has the same tendency with that of the population landscape.

Figure 11C, Figure 11F and Figure 11I show the heat dissipation rates decrease then increase when the parameter a_1, L_1, α increase. When the parameters $a_1=a_2=0.1$, $L_1=L_2=0.5$, $\alpha=1.0$, the system stays at a symmetrical landscape topography that the depths of the basin A and basin B have the same value. In this case, these two basins both have less contribution to the HDR since the flux in coexisting basin C is much larger than those in basin A or B. As the three parameters increase or decrease, one area of the basin A or B becomes generally more dominant than that of the symmetric landscape topography in addition to the area of basin C. Since the area of dominant flux expands, the heat dissipation rate becomes larger and the system needs to consume more energy.

Figure 12D and Figure 12F shows that the free energy increases as a_1 and α increase.Figure 12E shows the free energy increases as L_1 decreases. We can see there is no discontinuous changes in the first derivative of the free energy since there is no phase transition phenomenon.

Quantifying the kinetic paths for the non-equilibrium ecosystems

We showed the kinetic paths for the ecosystems on the landscapes(see the Materials and Methods section 3 for details). Figure 13A and Figure 13B show the kinetic paths on the intrinsic potential landscape ϕ_0 for competition model (We use the parameters $a_1=0.25$, $a_2=0.1$, $L_1=L_2=0.3$, $\alpha=1.0$ which has no coexisting state C in order to see the paths clearly here.) and for mutualism ($a_1=a_2=0.1$, $L_1=L_2=0.5$, $\alpha=1.0$) model respectively. Figure 13C and Figure 13D show the kinetic paths on the population potential landscape U for competition model and mutualism model with $D=0.01$. We can see the paths by purple line from state A and state B are quite different from the paths by black line from state B to A in Figure 13A and Figure 13C. The paths from A to C (from B to C) by purple line and the paths from C to A (from C to B)by black line are shown in Figure 13B and Figure 13D. We can see these pathways do not follow the gradient paths on both the intrinsic potential landscape and the population potential landscape due to the non-zero flux. The pathways do not necessarily pass the saddle point which is not similar with the equilibrium system. The forward and backward kinetic paths are irreversible which provides a clear signature of the non-equilibrium system. We can explore the detailed dynamical mechanism of ecosystems by quantifying the kinetic paths.

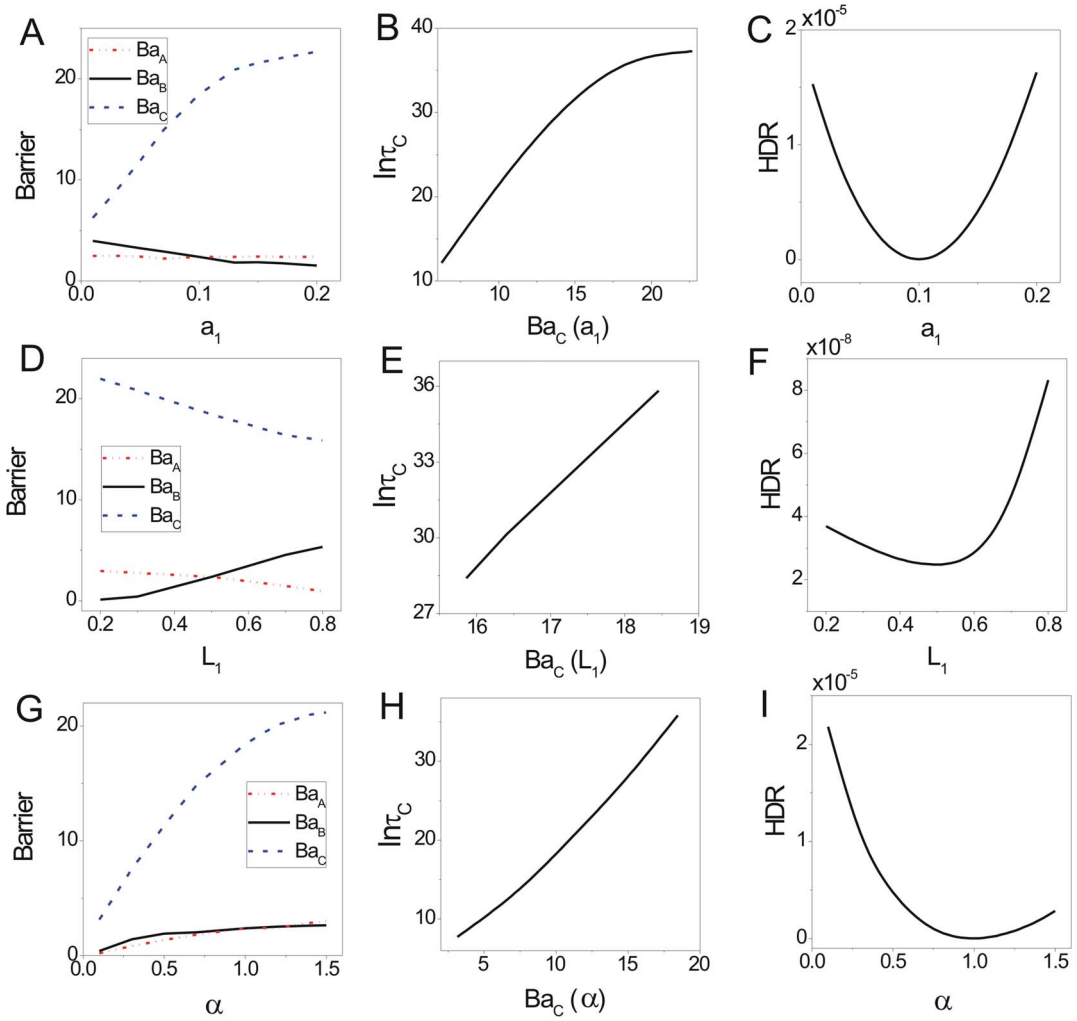

Figure 11. The barrier height of the population landscape, escape time and dissipation rate versus the rate parameters for mutualism model. (A) The barrier heights of the population landscape versus a_1. (B) The escape time versus barrier height of the population landscape for changing a_1. (C) The dissipation rate versus a_1. (D) The barrier height of the population landscape versus L_1. (E) The escape time versus barrier height of the population landscape for changing L_1. (F) The dissipation rate versus L_1. (G) The barrier height of the population landscape versus α. (H) The escape time versus barrier height of the population landscape for changing α. (I) The dissipation rate versus α.
doi:10.1371/journal.pone.0086746.g011

Quantifying the global stability and dynamics for Canada lynx and snowshoe hare population cycle

The lynx-snowshoe hare cycles show the typical predator-prey behaviors which many researches have tried to do realistic modeling on [2,22,23]. The modeling equations describing the behavior of lynx-snowshoe hare cycles were proposed and there exists limit cycles under much wider scope of parameters with consideration of the Holling-type II functional responses for lynx and Holling-type III functional responses for general predators, such as coyote and great horned owl in the boreal forest [2,22–24]. Here we use a model of lynx-snowshoe hare cycles shown as [22–24]: $\frac{dH}{dt} = rH(1-H/k) - \frac{\gamma H^2}{H^2+\eta^2} - \frac{\alpha HL}{H+\mu}$, $\frac{dL}{dt} = sL(1-qL/H)$, where H and L are the population density of hares and lynx. r is the growth rate of hares, k is the carrying capacity, γ is the maximum killing rate of general predation, η is the half-saturation constant for general predation [22–24]. α is the maximum killing rate of lynx, μ is the half-saturation constant for lynx' predation [22–24].

We can not ensure which oscillation is more robust by only the analysis of the local stability of differential equations. Therefore, we have explored the stochastic dynamics of this model and quantified the global stability using our landscape and flux theory. Figure 14A shows the population potential landscape with the basic set of parameters [22]. Figure 14B shows the sensitivity of each parameter with respect to the landscape topography through the barrier heights which can be used to quantify the robustness and global stability of the lynx-snowshoe hare cycles. The parameters decrease by $-20\%, -10\%, -5\%$ and increase by 5%, 10%, 20% of their own values. The color bars which are not displayed for each parameter, such as the disappearances of black and red bars for parameter r, indicate the disappearance of the periodical oscillations for that value of certain parameters. We can see the changing of r have significant impact on the robustness of the oscillation while the changes of the parameter γ and η have less significant impacts on the robustness of the oscillation. We showed a more detailed analysis of the robustness for changing parameter r in Figure 14C. There exists an optimal value r in Figure 14C. The optimal value of r leads to a more robust and stable ecological

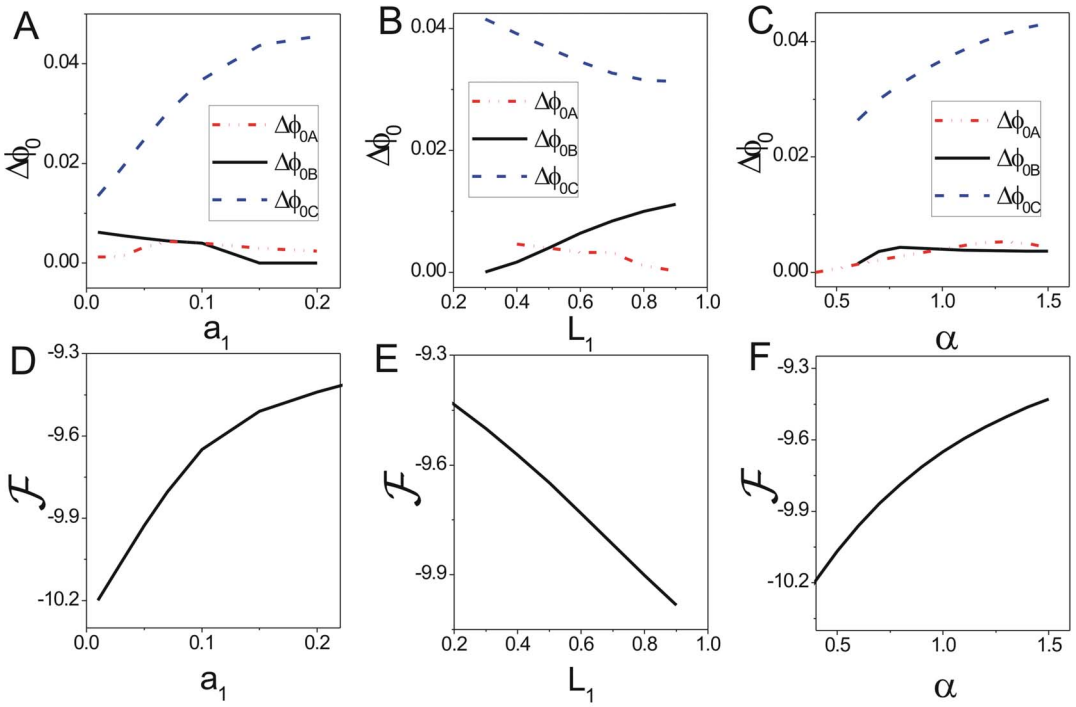

Figure 12. The barrier height of intrinsic potential landscape and free energy versus the rate parameters for mutualism model. The barrier heights of intrinsic potential landscape versus a_1 (A), L_1 (B), α (C). The free energy versus a_1 (D), L_1 (E), α (F).
doi:10.1371/journal.pone.0086746.g012

oscillation of hares and lynx. The barrier heights from the potential landscape topography can be used to quantify the global stability and the robustness of the oscillations. We can explore which set of parameters will lead the ecosystem to have more robust oscillation with higher barrier heights. This will help to design strategy to preserve the ecosystems.

Conclusion

Stability and dynamics are crucial for understanding the structure and function for ecology. Ecological stability is commonly defined as Lyapunov stability to describe the global stable behavior of ecosystem upon perturbations.Unfortunately, in general, Lyapunov stability cannot be assessed because explicit Lyapunov function can hardly be found. In this study we have illustrated a general method to explore the Lyapunov global stability of the ecosystem through the quantification of the underlying intrinsic landscape. It can be used to explore more general complex ecosystem where the situation can only be studied case by case before. We found the dynamics of the ecosystems is not only determined by the gradient of the potential landscape but also by an additional curl flux force from breaking down the detailed balance. This provides a new way to explore the general dynamics in non-equilibrium regime for ecosystems.

We considered three important ecological systems with the interactions between two species: the predation model, the competition model, the mutualism model and a realistic lynx-snowshoe hare model. Multiple attractors and limit cycle attractor with a distinct Mexican hat shape emerge from these cases. We found the quantitative measure for global stability through barrier height. The non-equilibrium free energy can reflect the global phases of the underlying ecosystems and the transition regions between the global phases. We quantified the pathways of ecosystem which do not follow the gradient path on the landscape and are irreversible. We quantified the kinetic speed from one stable state basin to another of the ecosystems and linked with the underlying landscape topography through the barrier height between the basins of attractions.

For ecosystems, the stability is directly related to the survivals of every species. We showed the effects of parameters representing the interactions among species on the global natures such as landscape topography represented by barrier height, kinetics speed represented by escape time and the thermodynamic dissipation by the entropy production or heat dissipation rate in these ecosystems. Therefore we can quantify the change of the stability by increasing or decreasing the interaction parameters, respectively. These results can help us to design more stable ecosystems.

The ecosystem dynamics shares some common global features as the biochemical systems such as gene-gene regulations, in terms of the underlying landscapes, the global stability and dynamics, kinetic rate and pathways. There are also significant differences between these two types of systems. First of all, the ecosystems and gene-gene regulation systems are at completely different level, one is on the population species and the other is within the cell. Second, their components have different sensitivity against changes. On the one hand, it is relatively easier to mutate the genes and harder to mutate the species. On the other hand, it is relatively easier to change the link between the species due to the sensitivity of ecosystems to the environment rather than the gene-gene regulations. Third, the ecosystems depend more sensitively to the outside input than the gene-gene regulations.

It is worth mentioning here that the landscape ecology is an emerging subfield in ecology. The landscape ecology models concentrate on spatial heterogeneity with space probabilistic methods [25,26]. Although these methods and our theory all focus on the dynamical evolution in probability, we concentrate on the probability landscape and flux in the population space rather than in the geographical space as in the landscape ecology models.

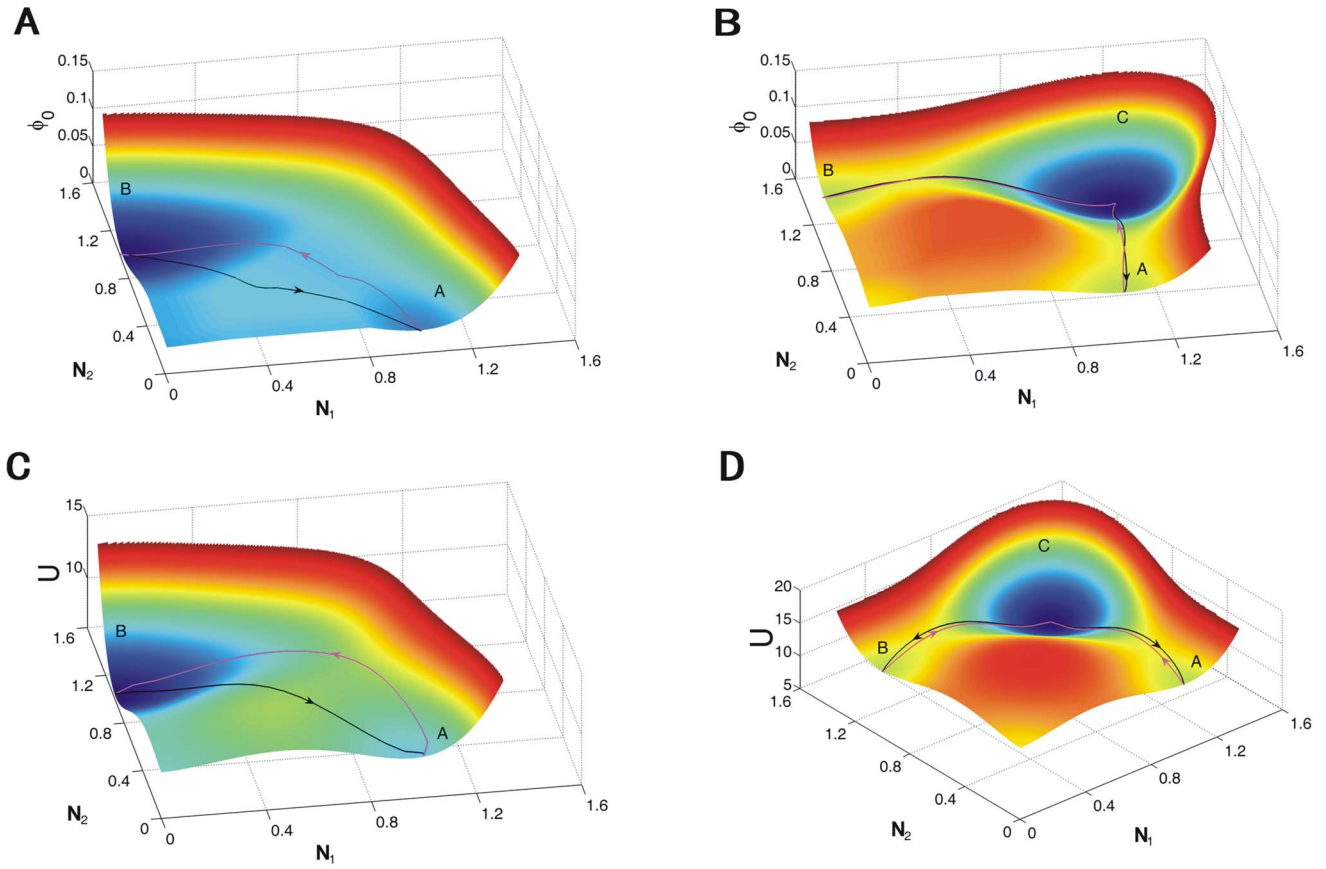

Figure 13. The paths for competition model and mutualism model. (A) The paths on the intrinsic potential landscape ϕ_0 for competition model. (B) The paths on the intrinsic potential landscape ϕ_0 for mutualism model. (C) The paths on the population potential landscape U for competition model. (D) The paths on the population potential landscape U for mutualism model.
doi:10.1371/journal.pone.0086746.g013

The realistic models are usually more complex. The models often have more parameters controlling the dynamical behaviors of the ecosystem. We can apply our potential and flux landscape framework to quantify the stability of those systems irrespect to how complicated the underlying processes dictated by the differential equations may be. Furthermore, we can explore the set of parameters for more stable system by the underlying landscape topography quantified by the barrier heights. Thus the parameter-control can be realized to achieve the ecological stability and ecological decision makings.

For a mutualism model like honeybee and flowering plants, the local analysis of the differential equations can only give the existence of the stable states and local stability but not the global robustness of the stable states. The honeybee and flowering plants can coexist in a wide range of their dynamical parameters. Our potential and flux landscape framework can give in which conditions the honeybee and flowering plants can more robustly coexist. We can also quantify the changes of the robustness of ecosystem through the changes in controlling parameters for the underlying landscape topography.

We can also use our potential and flux landscape theory to explore the interactions of multi-species as a multi-node network [15,27]. The analysis of sensitivity from the potential landscape can explore the effects of specific parameters or wirings to robustness and stability of the ecosystem. We can identify the key species or wirings that are responsible for the global stability and function of the whole ecosystem through the potential landscape topology.

The stability of ecosystems is a challenging issue. We have focused on our discussion with low dimensional models in this study. In realistic ecosystems, the global stability can seldomly be quantified by just exploring the stability with a few differential equations. The stability must be viewed as a multi-dimensional problem. It is determined by many internal and external degrees of freedom including population density, temperature, space, age,other competitors and environmental factors. A population dynamics P system (PDP) model as a tool for modeling and simulating complex ecosystems was proposed with a high computational modularity, efficiency, and the parallelism [28,29]. We will need to go further to explore the even more complex ecosystems with the consideration of other factors.

The methods developed in this study can be applied to more complicated and realistic ecosystems to understand the global stability, function and robustness.

Materials and Methods

Quantifying the non-equilibrium population and intrinsic potential, flux, Lyapunov function and non-equilibrium thermodynamics for general ecological systems with finite fluctuations

The ecological systems are not in isolations since there are often intrinsic and extrinsic environmental noises around them [30]. So

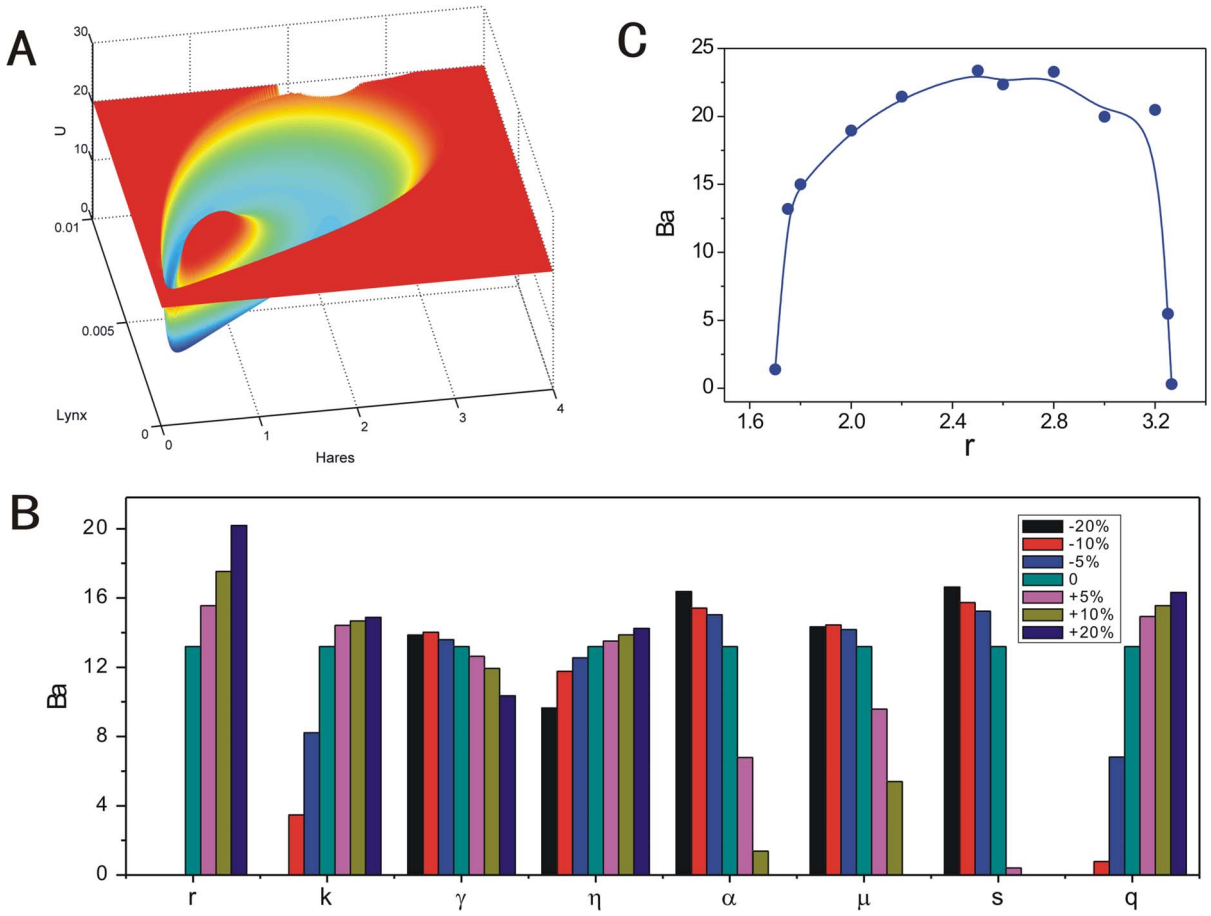

Figure 14. The potential landscape, barrier height of the population landscape and the sensitivity of parameters for lynx-snowshoe hare model. (A) The population potential landscape for lynx-snowshoe hare model. (B) The barrier heights versus changing parameters. The basic set of the parameters are: $r=1.75$, $k=8$, $\gamma=0.1$, $\eta=1.25$, $\alpha=505$, $\mu=0.3$, $s=0.85$, $q=212$. (C) The barrier heights versus the hares' rate of population growth.
doi:10.1371/journal.pone.0086746.g014

the dynamics can be described as follows [20,31]: $d\mathbf{N}/dt=\mathbf{F}(\mathbf{N})+\mathbf{g}\cdot\mathbf{\Gamma}$. The vector $\mathbf{F}(\mathbf{N})$ is the deterministic force that drives the system, where $\mathbf{N}$ is the vector of dynamical variables, with each component of which representing different species in the ecosystems. $\mathbf{g}$ is the noise force from the fluctuations. The statistical nature of the noise can often be assumed as Gaussian white noise: $<\mathbf{\Gamma}_i(t)\mathbf{\Gamma}_j(t')>=2D\delta_{ij}(t-t')$ ($\delta_{ij}=1$, if $i=j$; $\delta_{ij}=0$ if $i\neq j$) and $<\mathbf{\Gamma}_i(t)>=0$. D is the diffusion coefficient representing the level of noise strength while $\mathbf{G}=\mathbf{g}\cdot\mathbf{g}^T/2$ is the scaled diffusion matrix described the anisotropy phenomenon. We set $\mathbf{D}=D\mathbf{G}$.

Under fluctuations, the individual trajectories are stochastic and do not have the predictive power, we should focus on the evolution of probability distributions rather than evolution of individual trajectories. We can explore the corresponding stochastic dynamics governed by the Fokker-Planck diffusion equation [20,31] for the temporal evolution of the probability distribution $P(\mathbf{N},t)$:

$$\partial P/\partial t=-\nabla\cdot\mathbf{J}(\mathbf{N},t)=-\nabla\cdot(\mathbf{F}P-D\nabla(\mathbf{G}P)) \qquad (1)$$

This represents a conservation law of probability (local change is due to net flux in or out). The diffusion equation essentially describes the probability of finding the state $\mathbf{N}(t)$ in the state space which is driven by the driving force $\mathbf{F}$. The probability flux vector $\mathbf{J}$ of the system in population space $\mathbf{N}$ is defined as: $\mathbf{J}(\mathbf{N},t)=\mathbf{F}P-D\nabla(\mathbf{G}P)$.

In steady state, $\partial P/\partial t=0$, therefore $\nabla\cdot\mathbf{J}(\mathbf{N},t)=0$. $\mathbf{J}\neq 0$ means the detailed balance is broken and the ecosystem is in non-equilibrium state. The divergence-free property implies the flux $\mathbf{J}$ is rotational. From the definition of $\mathbf{J}(\mathbf{N},t)$, one can write the force decomposition: $\mathbf{F}=-D\mathbf{G}\nabla U+\mathbf{J}_{ss}/P_{ss}+D\nabla\cdot\mathbf{G}$. In this way, the driving force $\mathbf{F}$ can be decomposed into the gradient of the potential U, the divergence of the diffusion coefficient and the curl probability flux. Therefore the global nature can be determined by the non-equilibrium population potential U characterizing the probability landscape of the whole population space, the non-equilibrium local dynamics and their global properties can be determined by both the gradient of the potential landscape and the rotational curl flux [17]. This is in contrast with the zero flux case for detailed balance of equilibrium systems, where the global nature is determined by the equilibrium potential, and the dynamics is determined by the gradient of the equilibrium potential.

The steady state probability distribution under the fluctuation and the non-equilibrium population potential of ecosystems is quantitatively linked by: $P_{ss}(\mathbf{N})=\exp(-U)/Z$, where Z is the partition function for non-equilibrium ecosystems defined as $Z=\int\exp(-U)d\mathbf{N}$. Then the entropy of the non-equilibrium

ecosystem is given as [14,18,32–34]: $S=-\int P(\mathbf{N},t)\ln P(\mathbf{N},t)d\mathbf{N}$, and the energy of the non-equilibrium ecosystem is given as: $E=D\int UP(\mathbf{N},t)d\mathbf{N}=-D\int \ln[ZP_{ss}]P(\mathbf{N},t)d\mathbf{N}$. Therefore, the free energy $\mathcal{F}$ of the non-equilibrium ecosystem can be defined as:

$$\mathcal{F}=E-DS=D(\int P\ln(P/P_{ss})d\mathbf{N}-\ln Z). \quad (2)$$

The free energy is a combination of non-equilibrium energy and entropy, suggesting the first law of non-equilibrium thermodynamics for ecosystems. The free energy decreases in time monotonically until it reaches its minimum value, $\mathcal{F}=-D\ln Z$ [14,18,32–34]. The free energy of these non-equilibrium ecosystems never increases, suggesting the second law of non-equilibrium thermodynamics for ecosystems. We can use the free energy to explore the global stability of non-equilibrium ecosystems with finite fluctuations from the environments or intrinsic sources.

We also investigated the derivatives of the entropy in the time evolution [14,18,32–34]. It can be decomposed as follows:$\dot{S}=-\int (dP/dt)\, lnPd\mathbf{N}=\int (\mathbf{J}\cdot\mathbf{D}^{-1}\cdot\mathbf{J})/Pd\mathbf{N}-\int (\mathbf{J}\cdot\mathbf{D}^{-1}\cdot(\mathbf{F}-\nabla\cdot\mathbf{D}))d\mathbf{N}=\dot{S}_t-\dot{S}_e$ The first term is entropy production rate $\dot{S}_t$, having the physical significance of the total entropy change of system and environment. It is always non-negative corresponding to thermodynamic second law. The last term is the heat dissipation term $\dot{S}_e$ from the environments, and it can be either positive or negative [14,18,32–35]. The entropy of the ecosystems is not always increasing, but the free energy of the ecosystems reduces itself to a minimum in time. It can be used as an optimal principles to explore the topologies and the design of ecosystems.

Quantifying the non-equilibrium intrinsic potential and flux, Lyapunov function and global stability for general ecosystems with zero fluctuations: deterministic ecosystems

The essence of the stability-problem is to analyze that how a ecosystem returns to the original state under an initial perturbation. Lyapunov function is traditional used to quantify the global stability of dynamical ecosystems. But the population potential U we have obtained does not necessarily have the property of the Lyapunov function. [14–18, 32–34, 36–40]. Some analytical solutions of the Lyapunov function can be found for special simplified ecosystem models [5,8] and they can only be analyzed case by case. For complex real ecosystems, it is still challenging to find a proper Lyapunov function. We show here a general approach to obtain the Lyapunov functions for dynamical ecosystems.

The underlying intrinsic potential for the dynamic system can be obtained under the weak noise limit $D\ll 1$. Therefore, we can expand the population potential $U(\mathbf{N})$ according to the fluctuation strength D, and the associate probability $P(\mathbf{N})$ is as the following form [18,35,36,38,41]:

$$P(\mathbf{N})=\exp(-(\phi_0(\mathbf{N})/D+\phi_1(\mathbf{N})+D\phi_2(\mathbf{N})+\cdots))/Z \quad (3)$$

where $Z=\int \exp(-U(\mathbf{N}))d\mathbf{N}$. We can substitute the expanded equation to the Fokker-Plank diffusion equation.Therefore we have the D^{-1} order expansion of the Fokker-Plank diffusion equation: $H=\mathbf{F}\cdot\nabla\phi_0+\nabla\phi_0\cdot\mathbf{G}\cdot\nabla\phi_0=0$. The equation ϕ_0 followed is called Hamilton - Jacobi equation(HJE). We can solve the Hamilton-Jacobi equation which is zero-fluctuation limit of the Fokker-Planck equation to get the intrinsic potential ϕ_0 by a numerical method - level set method using the Mitchell's level-set toolbox [42].

Then we can study the deterministic equation for $\phi_0(\mathbf{N})$ [18,41]. We can explore the time evolution of the $\phi_0(\mathbf{N})$ in the zero fluctuation (D) limit:

$$\dot{\phi}_0(\mathbf{N})=\dot{\mathbf{N}}\cdot\nabla\phi_0=\mathbf{F}\cdot\nabla\phi_0=-\nabla\phi_0\cdot\mathbf{G}\cdot\nabla\phi_0\le 0 \quad (4)$$

Because $\mathbf{G}$ is positive definite, the value of $\phi_0(\mathbf{N})$ monotonously decreases under the deterministic evolution equation (zero fluctuation limit). Therefore ϕ_0 is a Lyapunov function, which can be used to quantify the global stability of the ecosystems. In addition, ϕ_0 is related to the population potential U under weak noise limit by $U=\phi_0/D$. So ϕ_0 is linked with the steady state probability which can quantify the global properties for ecosystem.

For the deterministic systems, we can take the zero-fluctuation limit and follow the procedures described above to obtain the non-equilibrium energy, entropy and free energy as well as the corresponding non-equilibrium thermodynamics. Furthermore, we can also recover the force decomposition for the deterministic ecosystems in zero fluctuation limit as gradient of non-equilibrium intrinsic potential $-\mathbf{G}\cdot\nabla\phi_0$ and steady state intrinsic divergent free curl flux $J_{ss}|_{D\to 0}$: $\mathbf{F}=-\mathbf{G}\cdot\nabla\phi_0+(\mathbf{J}_{ss}/P_{ss})|_{D\to 0}$.. From the Hamilton-Jacobian equation above, we see that $(\mathbf{J}_{ss}/P_{ss})|_{D\to 0}\cdot\nabla\phi_0=0$. This means the gradient of the non-equilibrium intrinsic potential ϕ_0 is perpendicular to the intrinsic flux under the zero-fluctuation limit [18,36,38].

Quantifying the paths of ecosystems

Quantification of the pathways of the ecosystems gives us an opportunity to explore the ecological dynamical process. We assume the path probability starts from initial configuration $\mathbf{N}_i$ at $t=0$, and end at the final configuration of $\mathbf{N}_f$ at time t. The path integral formula is [43,44]:

$$(\mathbf{N}_f,t|\mathbf{N}_i,0)=\int D\mathbf{N}exp[-\int L(\mathbf{N}(t))dt] \quad (5)$$

where L is the Lagrangian of the ecosystem [43,44]:

$$L=\frac{1}{4}D^{-1}(\dot{\mathbf{N}}-\mathbf{F})\cdot\mathbf{D}^{-1}\cdot(\dot{\mathbf{N}}-\mathbf{F})+\frac{1}{2}(\mathbf{D}\cdot\nabla)\cdot(\mathbf{D}^{-1}\cdot\mathbf{F}) \quad (6)$$

The path integral over $D\mathbf{N}$ represents the sum over all possible paths connecting $\mathbf{N}_i$ at time $t=0$ to $\mathbf{N}_f$ at time t. The term $(1/4)\ D^{-1}\ (\dot{\mathbf{N}}-\mathbf{F})\cdot\mathbf{D}^{-1}\cdot(\dot{\mathbf{N}}-\mathbf{F})$ gives the weight contribution from specific path from the underlying Gaussian noise. The term $(1/2)\ (\mathbf{D}\cdot\nabla)\cdot(\mathbf{D}^{-1}\cdot\mathbf{F})$ gives the contribution from the Jacobian variable transformation from the Gaussian noise to the path. The $L(\mathbf{N}(t))$ represents the weight for each path. The probability of ecosystem dynamics from initial configurations $\mathbf{N}_i$ to the final state $\mathbf{N}_f$ is equal to the sum of all possible paths with different weights. Not every dynamical path contributes to the same weight. We can identify the dominant paths which give the most contribution to the weight. This approximation is based on the fact the weight is exponentially weighted. The sub-leading contributions are exponentially small. Therefore dominant paths which give the most contribution to the weights can emerge. We explored the dominant kinetic paths from one state to another for ecosystems in this study.

The ecological dynamical models

The ecosystems can be described by a set of nonlinear ordinary differential equations for two species interactions. We will add some restrictions on the models to enable them to be more reasonable and closer to the real situation [2,45], such as avoidance of exponential growth and existence of lower critical bound for each species.

(1)Predation Model

The general Holling type II responses for the prey to account the nonlinearity in interactions can be added in a predation model proposed by Murray [2]:

$$\frac{dN_1}{dt}=N_1(1-N_1)-\frac{aN_1N_2}{N_1+d}=F_1(N_1,N_2)$$

$$\frac{dN_2}{dt}=bN_2(1-\frac{N_2}{N_1})=F_2(N_1,N_2) \quad (7)$$

where N_1 is the normalized population of prey while N_2 is the normalized population of predator.The parameter a is the relative death rate or the interaction strength for the prey. The parameter b is the ratio of the linear birth rate of the predator to that of the prey. The parameter d is the relative saturation rate of the prey. The system has two general saddle points: one is (0,0) representing that none of the species exists. The second one (1,0) represents the prey at their carrying capacity in the absence of predators [2]. The second point is stable along the N_1 population axis and unstable along the N_2 population axis. There is also a critical point which is the unstable center of the limit cycle or the stable point in different parameter ranges. The system has a stable limit cycle oscillation when we set $a=1.5$, $b=0.1$, $d=0.2$.

(2) Competition Model

The realistic competitive model should have with a lower critical bound, which means the creatures would perish once the size of the population is below this threshold. The model is shown as follows [45]:

$$\frac{dN_1}{dt}=N_1(N_1-L_1)(1-N_1)-a_1N_1N_2=F_1(N_1,N_2)$$

$$\frac{dN_2}{dt}=\alpha N_2((N_2-L_2)(1-N_2)-a_2N_1)=F_2(N_1,N_2) \quad (8)$$

where N_1 and N_2 are the normalized populations of the two competitive species S_A and S_B. L_1,L_2 are the lower critical bounds for species S_A,S_B, respectively. The ranges of L_1,L_2 are from 0 to 1. a_1,a_2 are the competitive ability for species S_A,S_B, respectively. α is the relative rate of natural increase for species S_B [45].

We have explored the phase analysis of the system. The two kinds of population which are both at zero mean the two species both are at extinct state (0,0) (Marked as O) of the system. This is because the two groups both have lower critical density. When there are no competitors for each species, the states: (1,0) (Marked as A, which means the species S_A exists alone.) and (0,1) (Marked as B, which means the species S_B exists alone.) that exist in isolation are locally stable. Besides the above three states, when the values of a_1 and a_2 meet certain conditions, the system can have another local stable state which corresponds to the coexistence of the two species (Marked as C). Here, we set $a_1=a_2=0.1$, $L_1=L_2=0.3$, $\alpha=1.0$ since it has these four states.

(3) Mutualism Model

We will consider the two mutualism species both having lower critical bound. This realistic mutualism model can be described as [45]:

$$\frac{dN_1}{dt}=N_1(N_1-L_1)(1-N_1)+a_1N_1N_2=F_1(N_1,N_2)$$

$$\frac{dN_2}{dt}=\alpha N_2((N_2-L_2)(1-N_2)+a_2N_1)=F_2(N_1,N_2) \quad (9)$$

where N_1 and N_2 are the normalized populations of the two mutualism species S_A and S_B. L_1,L_2 are lower critical points for species S_A and S_B, respectively. The ranges of L_1,L_2 are from 0 to 1. a_1,a_2 are the mutualism ability for species S_A,S_B, respectively. α is the relative rate of natural increasing for species S_B [45].

We have explored the phase analysis of this system. The two kinds of population which are both at zero mean the trivial solution (0,0) (Marked as O) of the system. This is because the two groups having a lower critical density. When there is no mutual helper for each species, the states: (1,0) (Marked as A, which means the species S_A exists alone.) and (0,1) (Marked as B,which means the species S_B exists alone.) that exist in isolation are locally stable. Besides the above three points, the system has another local stable point which corresponds to the coexistence of the two species (Marked as C). Here, we set $a_1=a_2=0.1$, $L_1=L_2=0.5$, $\alpha=1.0$ for the system has these four states completely.

Supporting Information

File S1 Supporting figures. **Figure S1.** The population potential landscapes for increasing diffusion coefficient D of predation model. **Figure S2.** The population potential landscapes for increasing parameter a of predation model.**Figure S3.** The population potential landscapes for increasing parameter b of predation model. **Figure S4.** The population potential landscapes for increasing parameter d of predation model. **Figure S5.** The population potential landscapes for increasing diffusion coefficient D of competition model. **Figure S6.** The population potential landscapes for increasing parameter a_1 of competition model. **Figure S7.** The population potential landscapes for increasing parameter L_1 of competition model. **Figure S8.** The population potential landscapes for increasing parameter α of competition model. **Figure S9.** The population potential landscapes for increasing diffusion coefficient D of mutualism model. **Figure S10.** The population potential landscapes for increasing parameter a_1 of mutualism model. **Figure S11.** The population potential landscapes for increasing parameter L_1 of mutualism model. **Figure S12.** The population potential landscapes for increasing parameter α of mutualism model.
(DOC)

Author Contributions

Conceived and designed the experiments: JW EKW. Performed the experiments: LX FZ. Analyzed the data: LX FZ KZ JW. Contributed reagents/materials/analysis tools: JW EKW. Wrote the paper: LX FZ JW EKW.

References

1. Vandermeer J, Goldberg D (2003) Population ecology: First principles. Woodstock, Oxfordshire: Princeton University Press.
2. Murray J (1998) Mathematical Biology. New York: Springer-Verlag Berlin Heidelberg.
3. Lotka A (1925) Elements of Physical Biology. Baltimore: Williams and Wilkins.
4. Volterra V (1931) Lecons sur la Theorie Mathematique de la Lutte pour la Vie. Paris: Gauthier- Villars.
5. Harrison G (1979) Global stability of predator-prey interactions. J Math Biology 8: 159–171.
6. Goh B (1976) Global stability in two species interactions. J Math Biol 3: 313–318.
7. Goh B (1977) Global stability in many-species systems. Am Nat 111: 135–143.
8. Hsu S (1978) On global stability of a predator prey system. Math Biosci 39: 1–10.
9. Holling C (1965) The functional response of predators to prey density and its role in mimicry and population regulation. Mem Ent Soc Can 45: 1–60.
10. Murdoch W, Oaten A (1975) Predation and population stability. Advan EcoL ReS 9: 1–131.
11. Hastings A (1978) Global stability of two species systems. J Math Biol 5: 399–403.
12. Balzsi G, van Oudenaarden A, Collins J (2011) Cellular decision making and biological noise: from microbes to mammals. Cell 144: 910–925.
13. Karsai I, Balzsi G (2002) Organization of work via a natural substance: regulation of nest con- struction in social wasps. J Theor Biol 218: 549–565.
14. Wang J, Huang B, Xia XF, Sun ZR (2006) Funneled landscape leads to robustness of cell networks: Yeast cell cycle. PloS Comput Biol 2: 1385–1394.
15. Han B, Wang J (2007) Quantifying robustness of cell cycle network: Funneled energy landscape perspectives. Biophys J 92: 3755–3763.
16. Lapidus S, Han B, Wang J (2008) Intrinsic noise, dissipation cost, and robustness of cellular networks: The underlying energy landscape of mapk signal transduction. Proc Natl Acad Sci USA 105: 6039–6044.
17. Wang J, Xu L, Wang EK (2008) Potential landscape and flux framework of nonequilibrium net- works: Robustness, dissipation, and coherence of biochemical oscillations. Proc Natl Acad Sci USA 105: 12271–12276.
18. Zhang F, Xu L, Zhang K, Wang E, Wang J (2012) The potential and flux landscape theory of evolution. J Chem Phys 137: 065102.
19. Xu L, Zhang F, Wang E, Wang J (2013) The potential and flux landscape, lyapunov function and non-equilibrium thermodynamics for dynamic systems and networks with an application to signal-induced ca2+ oscillation. Nonlinearity 26: 69–84.
20. Van Kampen N (2007) Stochastic processes in physics and chemistry. Amsterdam: Elsevier.
21. Yoda M, Ushikubo T, Inoue W, Sasai M (2007) Roles of noise in single and coupled multiple genetic oscillators. J Chem Phys 126: 1–11.
22. Tyson R, Haines S, Hodges K (2010) Modelling the canada lynx and snowshoe hare population cycle: the role of specialist predators. Theor Ecol 3: 97–111.
23. Krebs C, Boutin S, Boonstra R (2001) Ecosystem dynamics of the Boreal forest: the Kluane project. Oxford: Oxford University Press.
24. ODonoghue M, Boutin S, Krebs C, Zultea G, Murray D, et al. (1998) Functional responses of coyotes and lynx to the snowshoe hare cycle. Ecol 79: 1193–1208.
25. Wu J (2008) Landscape ecology. In: S. E. Jorgensen (ed), Encyclopedia of Ecology. Oxford: Elsevier.
26. Wu J, Hobbs R (2007) Key Topics in Landscape Ecology. Cambridge: Cambridge University Press.
27. Wang J, Li C, Wang E (2010) Potential and flux landscapes quantify the stability and robustness of budding yeast cell cycle network. Proc Natl Acad Sci USA 107: 8195–8200.
28. Colomer M, Margalida A, Perez-Jimenez M (2013) Population dynamics p system (pdp) models: A standardized protocol for describing and applying novel bio-inspired computing tools. PLoS ONE 8: e60698.
29. Colomer M, Margalida A, Sanuyc D, Perez-Jimenez M (2011) A bio-inspired computing model as a new tool for modeling ecosystems: The avian scavengers as a case study. Ecol Model 222: 33–47.
30. Swain P, Elowitz M, Siggia E (2002) Intrinsic and extrinsic contributions to stochasticity in gene expression. Proc Natl Acad Sci USA 99: 12795–12800.
31. Gillespie D (1977) Exact stochastic simulation of coupled chemical reactions. J Phys Chem 81: 2340–2361.
32. Ao P (2005) Laws in darwinian evolutionary theory. Phys Life Rev 2: 117–156.
33. Qian H (2009) Entropy demystified: The "thermo"-dynamics of stochastically uctuating systems. Method Enzymol 467: 111–134.
34. Schnakenberg J (1976) Network theory of microscopic and macroscopic behavior of master equation systems. Rev Mod Phys 48: 571–585.
35. Ge H, Qian H (2010) Physical origins of entropy production, free energy dissipation, and their mathematical representations. Phys Rev E 81: 051133.
36. Graham R (1989) Macroscopic potentials, bifurcations and noise in dissipative systems. In: Moss F, McClintock P, editors, Noise in Nonlinear Dynamical Systems Vol. 1, Cambridge University Press. pp. 225–278.
37. Sasai M, Wolynes PG (2003) Stochastic gene expression as a many-body problem. Proc Natl Acad Sci USA 100: 2374–2379.
38. Haken H (1987) Advanced synergetics: instability hierarchies of self-organizing systems and devices. Berlin: Springer.
39. Qian H (2006) Open-system nonequilibrium steady-state: Statistical thermodynamics, uctuations and chemical oscillations. J Phys Chem B 110: 15063–15074.
40. Qian H (2001) Mesoscopic nonequilibrium thermodynamics of single macromolecules and dynamic entropy-energy compensation. Phy Rev E 65: 016102.
41. Hu G (1986) Lyapunov function and stationary probability distributions. Z Phys B: Condens Matter 65: 103–106.
42. Mitchell IM (2008) The exible, extensible and efficient toolbox of level set methods. J Sci Comput 35: 300–329.
43. Wang J, Zhang K, Xu L, Wang E (2011) Quantifying the waddington landscape and biological paths for development and differentiation. Proc Natl Acad Sci USA 108: 8257–8262.
44. Wang J, Zhang K, Wang E (2010) Kinetic paths, time scale, and underlying landscapes: A path integral framework to study global natures of nonequilibrium systems and networks. J Chem Phys 133: 125103.
45. Bazykin A (1985) Mathematical Biophysics of Interacting Populations(in Russian). Moscow: Nauka.